

# Unprecedented Self-Organized Monolayer of a Ru(II) Complex by Diazonium Electroreduction

Van Quynh Nguyen,<sup>†,‡</sup> Xiaonan Sun,<sup>†</sup> Frédéric Lafalet,<sup>†,§</sup> Jean-Frédéric Audibert,<sup>⊥</sup> Fabien Miomandre,<sup>⊥</sup> Gilles Lemerrier,<sup>\*,||,†</sup> Frédérique Loiseau,<sup>§</sup> and Jean-Christophe Lacroix<sup>\*,†</sup>

<sup>†</sup>Univ. Paris Diderot, Sorbonne Paris Cité, ITODyS, UMR 7086 CNRS-15, rue Jean-Antoine de Baïf, 75205 Paris Cedex 13, France

<sup>‡</sup>Department of Advanced Materials Science and Nanotechnology, University of Science and Technology of Hanoi (USTH), Vietnam Academy of Science and Technology, 18 Hoang Quoc Viet, Cau Giay, Hanoi, Vietnam

<sup>§</sup>Département de Chimie Moléculaire, Université Grenoble-Alpes, CNRS UMR 5250, BP53, 38041 Grenoble, France

<sup>||</sup>Univ. Reims Champagne-Ardenne, Institut Chimie Moléculaire Reims, UMR 7312 CNRS, BP1039, 56187 Reims Cedex 2, France

<sup>⊥</sup>PPSM CNRS UMR8531, Ecole Normale Supérieure de Cachan, Université Paris-Saclay, 61 Avenue du Président Wilson, 94235 Cachan Cedex, France

## Supporting Information

**ABSTRACT:** A new heteroleptic polypyridyle Ru(II) complex was synthesized and deposited on surface by the diazonium electroreduction process. It yields to the covalent grafting of a monolayer. The functionalized surface was characterized by XPS, electrochemistry, AFM, and STM. A precise organization of the molecules within the monolayer is observed with parallel linear stripes separated by a distance of 3.8 nm corresponding to the lateral size of the molecule. Such organization suggests a strong cooperative process in the deposition process. This strategy is an original way to obtain well-controlled and stable functionalized surfaces for potential applications related to the photophysical properties of the grafted chromophore. As an exciting result, it is the first example of a self-organized monolayer (SOM) obtained using diazonium electroreduction.

There is a strong interest in the incorporation of ruthenium complexes onto ordered array systems for their potential use as building blocks in photoactive surfaces.<sup>1</sup> Advantages of the Ru(II) complexes in photochemistry and -physics reside in their unique combination of both chemical stability inertness, synthetic tailorability, and tunable electronic properties.<sup>2</sup> The long lifetimes of the triplet metal-to-ligand charge transfer excited state<sup>3</sup> (<sup>3</sup>MLCT, few ms<sup>4</sup>), is especially of interest for applications such as optical power limiting,<sup>5</sup> oxygen sensors,<sup>6</sup> and sensitizers.<sup>7</sup> Ru(II) complexes are also proposed as building blocks in molecular electronics<sup>8</sup> and widely used as dyes in solar cells.<sup>9</sup>

Ru(II) complexes have widely been deposited as thin films by spin-coating<sup>10</sup> or by incorporation in a conductive polymer matrix.<sup>11</sup> Monolayers have also been obtained using the Langmuir–Blodgett method or specific complexes bearing thiol-anchoring groups and SAM-based techniques.<sup>12</sup> Covalent grafting of Ru(II) complexes using diazonium electroreduction was also investigated.<sup>13</sup> Functionalization of surfaces via this process is now well-known.<sup>14</sup> It can be performed with molecules bearing several functional groups and usually leads to

disorganized multilayers with film thickness around 5 nm.<sup>14</sup> Generation of monolayers using diazonium electroreduction is still considered as a major challenge. Several strategies have been proposed for this purpose. The first one<sup>15</sup> was based on the use of the bulky 3,5-bis-*t*-butylaniline groups. It was shown that the electroreduction of the corresponding diazonium leads to a monolayer, thanks to steric effect. Other approaches to obtain monolayers are the use of (i) diazonium derivatives with protective groups, which are removed in a postfunctionalization step;<sup>16</sup> (ii) ionic liquids;<sup>17</sup> (iii) a radical scavenger in the solution.<sup>18</sup> Note also that new methods to generate monolayers on various surfaces have recently been introduced.<sup>19</sup>

In this work, a new heteroleptic Ru(II) complex [Ru-(bpyFluo)<sub>2</sub>(bpyNH<sub>2</sub>)]<sup>2+</sup> (**1**, see Figure 1, left for the representation

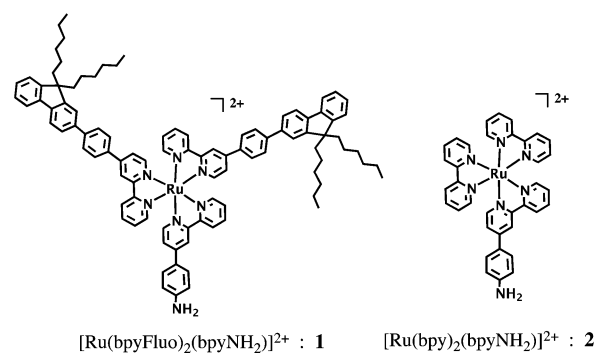


**Figure 1.** Molecular structure of compound **1** and parent complex **2**.

of one of the isomers), involving 5-substituted-2,2'-bipyridine-based ligands was synthesized starting from RuCl<sub>3</sub>, the already described compound **bpyNH<sub>2</sub>**<sup>13a</sup> and the new **bpyFluo** ligand (see Supporting Information (SI) for the synthesis and characterizations). It was designed so that the bulky groups attached to the 2,2'-bipyridine core ligands may limit the thickness of the deposited layer.<sup>15</sup> The electroreduction of the *in*

Received: May 24, 2016

Published: July 18, 2016

*situ* chemically generated diazonium was performed and yielded to ultrathin modified layers characterized by AFM, XPS, and electrochemistry. Thickness measurements by several means and STM studies were performed in order to investigate the organization of the deposited layer.

Fluorine groups added new photophysical properties to the Ru-based complexes; the molecular properties of complex **1** were first studied and compared to the parent complex **2**. The absorption spectrum of complex **1** (Figure 2-a) is composed of

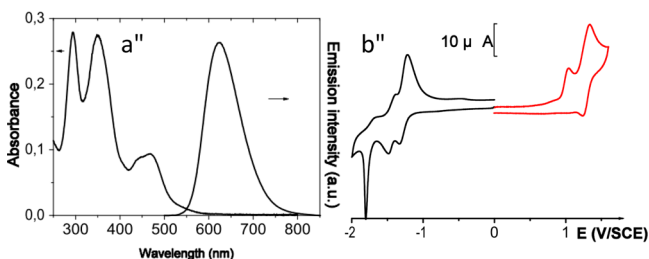


**Figure 2.** (a) Absorption and emission spectrum of a CH<sub>3</sub>CN solution of **1**. (b) Cyclic voltammetry of a millimolar solution of **1** in CH<sub>3</sub>CN + TBAPF<sub>6</sub> (10<sup>-1</sup> M) on GC electrode at  $\nu = 100 \text{ mV}\cdot\text{s}^{-1}$ .

(i) two intense bands centered at 295 and 350 nm, which are mainly attributed to  $\pi-\pi^*$ , and intraligand charge-transfer (ILCT) transition, respectively (ILCT involves a charge flow from the fluorine units to the pyridyle moiety); (ii) a broad band between 400 and 550 nm, which corresponds to  $d(\text{Ru}^{2+}) \rightarrow \pi^*$ -metal-to-ligand charge-transfer (<sup>1</sup>MLCT) transitions.<sup>20</sup> The classical emission centered at 625 nm is due to the radiative de-excitation of the lowest-lying <sup>3</sup>MLCT excited-state,<sup>3</sup> more probably directed toward a fluorine-substituted bipyridine ligand, which is easier to reduce than the aniline-substituted one.

Compared to the parent complex **2**,<sup>13</sup> emission quantum yield ( $\phi_{\text{em}}$ ) and excited-state lifetime ( $\tau$ ) in deaerated acetonitrile solution were improved ( $\phi_{\text{em}} = 8.7\%$  and  $4.1\%$ ,  $\tau = 1.2$  and  $0.7 \mu\text{s}$ , for **1** and **2**, respectively). Involvement of the fluorine moiety in the delocalization of the excitation state was confirmed by time-resolved transient absorption spectrum. An intense and very broad feature appears between 520 and 750 nm and is actually due to the important delocalization and stabilization of the radical anion in the substituted ligand (see Figure S2) as already reported for Ru(bpy)<sub>3</sub><sup>2+</sup> moieties connected to conjugated polyphenylene chains.<sup>21</sup>

The electrochemical behavior of a millimolar solution of **1** (CH<sub>3</sub>CN + 0.1 M TBAP) has been studied by cyclic voltammetry on glassy carbon electrode in the  $-2/1.5 \text{ V}$  potentials window. The response of the Ru complex exhibits two successive anodic waves (Figure 2b) accounting for one-electron transfers at  $E_{\text{pa}} = 1 \text{ V/SCE}$  and  $E_{1/2} = 1.28 \text{ V/SCE}$  ( $\Delta E_{\text{p}} = 100 \text{ mV}$ ) corresponding to the irreversible aniline oxidation and to the reversible ruthenium metal center oxidation. In the region of negative potentials, the curve displays three one-electron partially reversible cathodic waves at  $E_{1/2} = -1.33, -1.5, \text{ and } -1.88 \text{ V/SCE}$  corresponding to the reduction of the bipyridine ligands.

The diazonium salt derived from complex **1** has been *in situ* generated adding 15 equiv of *tert*-butylnitrite (*t*-BuNO<sub>2</sub>). Figure S3 shows successive cycles of its electrochemical reduction between 0.4 and  $-0.6 \text{ V/SCE}$ . In the first cycle, an irreversible peak at  $E_{\text{pc}}$  close to  $0 \text{ V/SCE}$ , characteristic of the diazonium reduction, is observed. In the next cycles, the CVs show a dramatic decrease in the peak current, which almost disappears after a few cycles. These observations suggest that complex **1** has been grafted onto

the surface, which was confirmed by the X-ray photo electron spectroscopy (XPS) analysis of the surface.<sup>12</sup> The peaks attributed to the ITO substrate (tin and indium oxide) are still observed, which indicates that the film thickness is below 10 nm. Furthermore, the nitrogen signal is stronger than on the initial ITO electrode, and one new peak at 281.2 eV attributed to Ru(II) 3d<sub>5/2</sub> (Ru(II) 3d<sub>3/2</sub>, at 285.4 eV is masked by C<sub>1s</sub> signal) is observed. The ratios between Ru and C and between Ru and N are in good agreement with theoretical values. These quantitative results (see SI for data) confirm that a thin film of the Ru(II) complex **1** has been grafted onto the surface.

The effective anchorage of the complex onto ITO was also checked by cyclic voltammetry restricted to the oxidative process centered on the Ru-center. The CV curve of Ru(bpyFluo)<sub>2</sub>bpy<sup>2+</sup> (**1**) on ITO shows the expected reversible oxidation wave at  $E_{1/2} = 1.23 \text{ V}$  ( $\Delta E_{\text{p}} \approx 0 \text{ V}$  at low scan rates). The shape of this wave is characteristic of immobilized electroactive species. Increasing the number of cycles used during the layer deposition process did not lead to an increase of the amount of deposited units as no apparent increase of the film electroactivity was evidenced. Integration of the Ru<sup>3+/2+</sup> redox peaks recorded yields an apparent surface concentration of  $5.2 \times 10^{-10} \text{ mol}\cdot\text{cm}^{-2}$ , which is close to that of a monolayer.<sup>22</sup> Stability of the deposited film is very good as it can be reversibly swept up to 1.4 V without any loss of the Ru<sup>3+/2+</sup> signal.

We measured the thickness of the layers grown on ITO with an increasing number of cycles, between 0.4 and  $-0.6 \text{ V/SCE}$  by atomic force microscopy (AFM) using two methods. The first one is based on AFM topography images of a scratch in the films (see Figure S6). A homogeneous coverage can be observed with a high contrast between the inner and outer zones of the scratch. The corresponding depth profiles (see SI) show that, when the modified electrode is prepared with 5 grafting cycles, the average film thickness is  $2 \pm 0.5 \text{ nm}$ , whereas when the number of cycle increases to 30 cycles, the average film thickness increases slightly and reaches  $2.5 \pm 0.5 \text{ nm}$ , with a roughness of  $\sim 0.5 \text{ nm}$ . These thicknesses were confirmed by a nondestructive method. It combines diazonium electroreduction and nanosphere lithography.<sup>23</sup> This method generates nanostructured surfaces with well-organized nanoholes in a honeycomb organization. AFM can then be used for measuring the depth of these holes. Figure 3a shows an AFM image of such structures, whereas Figure 3c shows the profile corresponding to the white line through four neighboring holes. The average hole depth is 2.5–3 nm. This result is similar to that previously deduced using the scratch

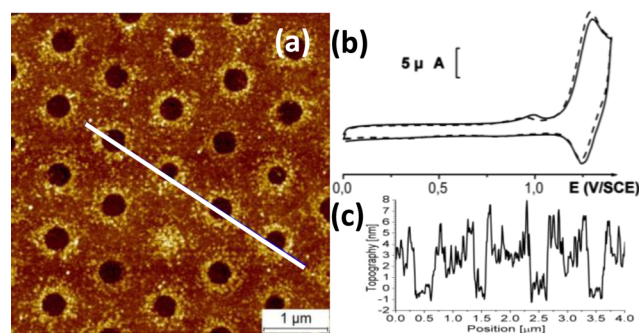


**Figure 3.** (a) Honeycomb structures of nanoholes in an ultrathin film of [Ru(II)] complex **1** deposited on ITO. (b) CV of electrografted film on ITO in CH<sub>3</sub>CN + 0.1 M TBAPF<sub>6</sub> after 15/30 cycles. (c) Profile corresponding to the white line in panel a, through four neighboring holes.

method and clearly demonstrates the presence of a monolayer of complex **1** grafted on the ITO surface. It also suggests that, in the configuration used here, the layer growth is sterically blocked, whereas multilayer formation was reported for the parent complex **2**.<sup>13</sup>

This monolayer was then studied using scanning tunneling microscopy (STM). Details on the STM setup can be found in the SI files. To do so, the same electrografting method was applied to deposit complex **1** on highly ordered pyrolytic graphite (HOPG). A monolayer is again obtained as evidenced by STM. This technique reveals a short-range self-organization of the molecules in the monolayer (Figure 4a), which develops on

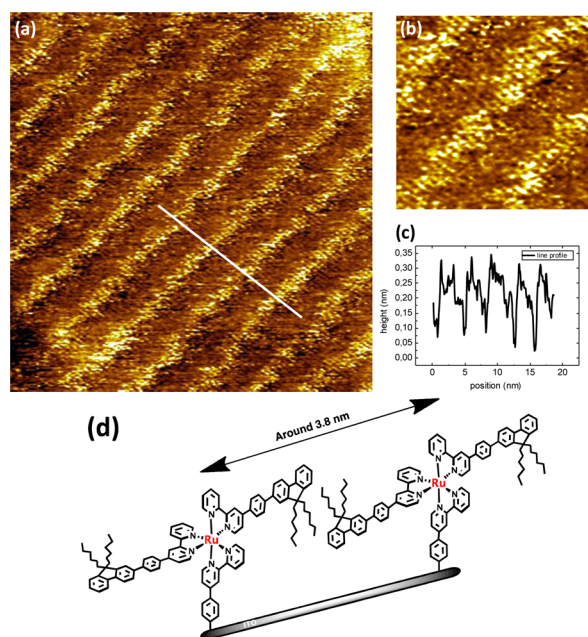


**Figure 4.** (a) STM image of complex **1** grafted on HOPG:  $33 \times 30 \text{ nm}^2$ ,  $I_t = 13 \text{ pA}$ ,  $V_s = -350 \text{ mV}$ . (b) STM image,  $11 \times 11 \text{ nm}^2$ . (c) Line profile of monolayer molecular stripes. (d) Proposed scheme for the [Ru(II)] complexes in supramolecular side-by-side organization.

the HOPG terraces and is highly reproducible. It is not observed upon spontaneous grafting, and only occurs from electrochemical reduction of complex **1** diazonium. The HOPG surface is fully covered with parallel stripes. They exhibit nonlinear defects revealing small shifts of adjacent molecules as depicted in the SI files. The in-plane spacing between the nearest neighboring stripes, determined by an STM cross-section, is  $3.8 \pm 0.5 \text{ nm}$  (see Figure 4c, statistic on 5 samples). The  $\pm 0.5 \text{ nm}$  error is contributed from both the variation of neighboring stripes spacing and the STM piezoelectric drift. This value matches the molecular length of **1**. Parallel straight bright lines are resolved from inside the molecular stripes with a submolecular resolution (see Figure 4b). The intramolecular bright lines are oriented in a direction perpendicular to the stripe main axes and, due to the electronic coupling between the chemisorbed Ru-core and the substrate, may involve more directly the Ru-bpy core.<sup>12b,c</sup>

A side-by-side molecular structure may explain the complex **1** supra-molecular organization (see Figure 4d). Three-dimensional  $[\text{Ru}(\text{bpyFluo})_2\text{bpy}]^{2+}$  entities are packed in parallel side-by-side forming the supramolecular stripe and are “standing” protruded out of plane to the substrate surface. The Ru(II) complexes are stabilized in ordered stripe patterns probably from

a balanced competition between molecule–substrate chemisorption and an intermolecular  $\pi$ – $\pi$  (or other low energy interactions) stacking. Several domains showing the same nanostripe organization are observed by STM with clear separations (see Figure S7 in SI). The rotating angles from the different domains are always with value times of  $60^\circ$ . This indicates that there is a unit structure from the self-organization of complex **1** and the domain separation is induced by the 3-fold symmetry of the HOPG substrate.

Monolayer organizations are usually observed with two kinds of molecule/substrate interaction. Planar molecules self-assembled from physisorption<sup>24</sup> and thiol-based SAM on gold<sup>25</sup> in which the reaction between the molecule and the surface is reversible and progressive reorganization of the surface is possible. However, it has never been observed with layers generated from diazonium chemistry in which chemisorption involving strong covalent bonds occurs. Indeed, steric effects, on the density of covalent grafting using diazonium chemistry were recently demonstrated in an unprecedented way by STM but long-range organization were not observed.<sup>26</sup> It is likely that in the present case a first covalently bounded molecular complex acts as a seeding agent giving a nucleation point for subsequent elongation of ordering, involving cooperative effects and efficient supramolecular interactions with the “next” complex in solution.<sup>27</sup>

The photophysical properties of the grafted Ru complex **1** were investigated using time-resolved fluorescence microscopy. The excited state lifetime was measured to be 23 ns, which is much shorter than for the free complex,<sup>4</sup> showing a quenching by the ITO surface. The electrofluorochromic behavior of the grafted complex could also be evidenced when applying potential steps leading to the switch of the Ru center redox state (see Figure S10B in SI). A clear modulation of the luminescence recorded above 530 nm (see emission spectrum in Figure S10A) can be seen in phase with the potential modulation showing that the electrofluorochromic properties of such complex<sup>28</sup> are retained on the surface.

To summarize, we report here the first example of a Ru(II) complex, which gives a monolayer during electroreduction of the related diazonium salt on ITO and HOPG. The molecules in the monolayer are locally organized when deposited on HOPG as evidenced by STM, with parallel molecular stripes covering the terraces of the HOPG surface. The in-plane spacing between the nearest neighboring stripes is  $3.8 \pm 0.5 \text{ nm}$ , matching the lateral size of the complex and revealing a fingerprint of the molecular packing. This layer can be seen as a “Ru(II)-complex skin” on the surface with potential applications related to its photophysical properties. A molecular engineering and theoretical approach is currently under investigation in our group, for a better understanding of this unprecedented, rapid and robust 2D self-organization of a monolayer of such 3D molecular structures.

## ■ ASSOCIATED CONTENT

### 📄 Supporting Information

The Supporting Information is available free of charge on the ACS Publications website at DOI: 10.1021/jacs.6b04827.

Molecular synthetic procedures and electrografting methods; electrochemical and microscopic characterization details (PDF)

## ■ AUTHOR INFORMATION

## Corresponding Authors

\*lacroix@univ-paris-diderot.fr

\*gilles.lmercier@univ-reims.fr

## Notes

The authors declare no competing financial interest.

## ■ ACKNOWLEDGMENTS

ANR are gratefully acknowledged for their financial support of this work (ANR 11 LABX 086, ANR 11 IDEX 05 02, ANR-11-LABX-0003-01).

## ■ REFERENCES

- (1) Forster, R. J.; Keyes, T. E. *Coord. Chem. Rev.* **2009**, *253*, 1833–1853.
- (2) Coe, B. J. *Acc. Chem. Res.* **2006**, *39*, 383–393.
- (3) Campagna, S.; Puntoriero, F.; Nastasi, F.; Bergamini, G.; Balzani, V. *Top. Cur. Chem.* **2007**, *280*, 117–214.
- (4) Caspar, J. V.; Meyer, T. J. *J. Am. Chem. Soc.* **1983**, *105*, 5583–5590.
- (5) (a) Humphrey, M. G.; Lockhart-Gillet, B.; Samoc, M.; Skelton, B. W.; Tolhurst, V.-A.; White, A. H.; Wilson, A. J.; Yates, B. F. *J. Organomet. Chem.* **2005**, *690*, 1487–1497. (b) Four, M.; Riehl, D.; Mongin, O.; Blanchard-Desce, M.; Lawson-Daku, L. M.; Moreau, J.; Chauvin, J.; Delaire, J. A.; Lemerrier, G. *Phys. Chem. Chem. Phys.* **2011**, *13*, 17304–17312.
- (6) Elias, B.; Kirsch-De Mesmaeker, A. *Coord. Chem. Rev.* **2006**, *250*, 1627–1641.
- (7) (a) Liu, Y.; Hammitt, R.; Lutterman, D. A.; Joyce, L. E.; Thummel, R. P.; Turro, C. *Inorg. Chem.* **2009**, *48*, 375–385. (b) Boca, S.; Four, M.; Bonne, A.; van Der Sanden, B.; Astilean, S.; Baldeck, P. L.; Lemerrier, G. *Chem. Commun.* **2009**, 4590–4592.
- (8) (a) Sauvage, J.-P.; Collin, J.-P.; Chambron, J. C.; Guillerez, S.; Coudret, C.; Balzani, V.; Barigelletti, F.; De Cola, L.; Flamigni, L. *Chem. Rev.* **1994**, *94*, 993–1019. (b) Winter, A.; Hoepfner, S.; Newkome, G. R.; Schubert, U. S. *Adv. Mater.* **2011**, *23*, 3484–3498.
- (9) Hagfeldt, A.; Boschloo, G.; Sun, L.; Kloo, L.; Pettersson, H. *Chem. Rev.* **2010**, *110*, 6595–6663.
- (10) Gao, F. G.; Bard, A. J. *J. Am. Chem. Soc.* **2000**, *122*, 7426–7427.
- (11) (a) Bidan, G.; Deronzier, A.; Moutet, J. C. *New J. Chem.* **1984**, *8*, 501–503. (b) Reuillard, B.; Le Goff, A.; Cosnier, S. *Anal. Chem.* **2014**, *86*, 4409–4415.
- (12) (a) Vergeer, F. W.; Chen, X.; Larolet, F.; De Cola, L.; Fuchs, H.; Chi, L. *Adv. Funct. Mater.* **2006**, *16*, 625–632. (b) Figgemeier, E.; Merz, L.; Hermann, B. A.; Zimmermann, Y. C.; Housecroft, C. E.; Guntherodt, H.-J.; Constable, E. C. *J. Phys. Chem. B* **2003**, *107*, 1157–1162. (c) Schramm, A.; Stroh, C.; Dössel, K.; Lukas, M.; Fuhr, O.; Löhneysen, H.; Mayor, M. *Chem. Commun.* **2013**, *49*, 1076–1078. (d) Madueno, R.; Räisänen, M. T.; Silien, C.; Buck, M. *Nature* **2008**, *454*, 618–621. (e) De La Llave, E.; Herrera, S. E.; Mendez De Leo, L. P.; Williams, F. J. *J. Phys. Chem. C* **2014**, *118*, 21420–21427.
- (13) (a) Jousset, B.; Bidan, G.; Billon, M.; Goyer, C.; Kervella, Y.; Guillerez, S.; Abou Hahad, E.; Goze-Bac, C.; Mevellec, J. Y.; Lefrant, S. *J. Electroanal. Chem.* **2008**, *621*, 277–285. (b) Agnès, C.; Arnault, J.-C.; Omnès, F.; Jousset, B.; Billon, M.; Bidan, G.; Mailley, P. *Phys. Chem. Chem. Phys.* **2009**, *11*, 11647–11654. (c) Piper, D. J. E.; Barbante, G. J.; Brack, N.; Pigram, P. J.; Hogan, C. F. *Langmuir* **2011**, *27*, 474–480.
- (14) (a) Pinson, J.; Podvorica, F. *Chem. Soc. Rev.* **2005**, *34*, 429–439. (b) Stockhausen, V.; Ghilane, J.; Martin, P.; Trippé-Allard, G.; Randriamahazaka, H.; Lacroix, J. C. *J. Am. Chem. Soc.* **2009**, *131*, 14920–14927.
- (15) Combellas, C.; Kanoufi, F.; Pinson, J.; Podvorica, F. I. *J. Am. Chem. Soc.* **2008**, *130*, 8576–8577.
- (16) (a) Leroux, Y. R.; Fei, H.; Noël, J.-M.; Roux, C.; Hapiot, P. *J. Am. Chem. Soc.* **2010**, *132*, 14039–14041. (b) Malmos, K.; Dong, M.; Pillai, S.; Kingshott, P.; Besenbacher, F.; Pedersen, S. U.; Daasbjerg, K. *J. Am. Chem. Soc.* **2009**, *131*, 4928–4936. (c) Lee, L.; Leroux, Y. R.; Hapiot, P.; Downard, A. J. *Langmuir* **2015**, *31*, 5071–5077. (d) Lee, L.; Gunby, N. R.; Crittenden, D. L.; Downard, A. L. *Langmuir* **2016**, *32*, 2626–2637.
- (17) Fontaine, O.; Ghilane, J.; Martin, P.; Randriamahazaka, H.; Lacroix, J.-C. *Langmuir* **2010**, *26*, 18542–18549.
- (18) (a) Menanteau, T.; Levillain, E.; Breton, T. *Chem. Mater.* **2013**, *25*, 2905–2909. (b) Menanteau, T.; Levillain, E.; Breton, T. *Langmuir* **2014**, *30*, 7913–7918.
- (19) (a) Horton, J. H.; Ebraldize, I. I.; Zenkina, O. V.; McLean, A. B.; Drevniok, B.; She, Z.; Kraatz, H.-B.; Mosey, N. J.; Seki, T.; Keske, E. C.; Leake, J. D.; Rousina-Webb, A.; Wu, G. *Nat. Chem.* **2014**, *6*, 409–414. (b) Zaba, T.; Noworolska, A.; Morris Bowers, C.; Breiten, B.; Whitesides, G. M.; Cyganik, P. *J. Am. Chem. Soc.* **2014**, *136*, 11918.
- (20) Girardot, C.; Lemerrier, G.; Mulatier, J.-C.; Chauvin, J.; Baldeck, P. L.; Andraud, C. *Dalton Trans.* **2007**, *31*, 3421–3426.
- (21) Welter, S.; Larolet, F.; Cecchetto, E.; Weerger, F.; De Cola, L. *ChemPhysChem* **2005**, *6*, 2417–2427.
- (22) Brooksby, P. A.; Downard, A. J. *Langmuir* **2004**, *20*, 5038–5045.
- (23) (a) Maldonado, S.; Smith, T. J.; Williams, R. D.; Morin, S.; Barton, E.; Stevenson, K. J. *Langmuir* **2006**, *22*, 2884–2891. (b) Corgier, B. P.; Bélanger, D. *Langmuir* **2010**, *26*, 5991. (c) Santos, L.; Ghilane, J.; Lacroix, J.-C. *Electrochem. Commun.* **2012**, *18*, 20–23. (e) Santos, L.; Martin, P.; Ghilane, J.; Lacaze, P. C.; Lacroix, J.-C. *ACS Appl. Mater. Interfaces* **2013**, *5*, 10159–10164.
- (24) (a) Barth, J. V. *Annu. Rev. Phys. Chem.* **2007**, *58*, 375–407. (b) Destoop, I.; Ghijssens, E.; Katayama, K.; Tahara, K.; Mali, K. S.; Tobe, Y.; De Feyter, S. *J. Am. Chem. Soc.* **2012**, *134*, 19568–19571. (c) Tahara, K.; Yamaga, H.; Ghijssens, E.; Inukai, K.; Adisoejoso, J.; Blunt, M. O.; De Feyter, S.; Tobe, Y. *Nat. Chem.* **2014**, *6*, 1024. (d) Silly, F.; Kervella, Y.; Jousset, B. *RSC Adv.* **2015**, *5*, 101740–101744. (e) Rajwar, D.; Sun, X.; Cho, S. J.; Grimsdale, A. C.; Fichou, D. *CrystEngComm* **2012**, *14*, 5182–5187.
- (25) Tour, J. M.; Jones, L. R.; Pearson, D. L.; Lamba, J. J. S.; Burgin, T. P.; Whitesides, G. M.; Allara, D. L.; Parikh, A. N.; Atre, S. *J. Am. Chem. Soc.* **1995**, *117*, 9529–9534.
- (26) Greenwood, J.; Phan, T. H.; Fujita, Y.; Li, Z.; Ivasenko, O.; Vanderlinden, W.; Gorp, H. V.; Frederickx, W.; Lu, G.; Tahara, K.; Tobe, Y.; Uji-I, H.; Mertens, S. F. L.; De Feyter, S. *ACS Nano* **2015**, *9*, 5520–5535.
- (27) Frath, D.; Sakano, T.; Imaizumi, Y.; Yokoyama, S.; Hirose, T.; Matsuda, K. *Chem. - Eur. J.* **2015**, *21*, 11350–11358.
- (28) Miomandre, F.; Pansu, R. B.; Audibert, J. F.; Guerlin, A.; Mayer, C. R. *Electrochem. Commun.* **2012**, *20*, 83–87.